SUPPLEMENTAL MATERIALS

AIP1 functions as Arf6-GAP to negatively regulate TLR4 signaling

Ting Wan[1,2*], Ting Liu[1*], Haifeng Zhang[1], Shibo Tang[2,3], and Wang Min[1,2,3]

[1]Interdepartmental Program in Vascular Biology and Therapeutics, Department of Pathology, Yale University School of Medicine, 10 Amistad St., New Haven, CT 06520. [2]State Key Laboratory of Ophthalmology, Zhongshan Ophthalmic Center, Sun Yat-Sen University, Guangzhou, China

[3]Corresponding author: Dr. Wang Min, Interdepartmental Program in Vascular Biology and Therapeutics and Department of Pathology, Yale University School of Medicine, 10 Amistad St., New Haven, CT 06520. Tel: 203-785-6047; Fax: 203-737-2293; Email: wang.min@yale.edu; Shibo Tang Zhongshan Ophthalmic Center, Sun Yat-Sen University, Guangzhou, China. tangsb@mail.sysu.edu.cn.

.

* These authors contribute to this work equally.

Supplemental Figures

Fig.S1. Effects of AIP1 on IL-1R, TLR4 and TLR2 signaling. a. Effects of AIP1 on IL-1β-induced NF-κB and MAPK activation in MLEC. WT and AIP1-KO MLEC ($1X10^6$) were treated with IL-1β (10 ng/ml) for the indicated times. Phospho- and total IκBβ and p38 were determined by immunoblotting with the respective antibodies. **b**. Effects of AIP1 in TLR4-mediated NF-κB signaling. WT and AIP1-KO MLEC were pre-treated with protein synthesis inhibitor cylcoheximide (10 mg/ml) for 60 min followed by stimulation with LPS (1 ng/ml) for the indicated times. Phospho- and total IκBβ were determined by immunoblotting with the respective antibodies. **c.** Effects of AIP1 on TLR2-induced NF-κB and MAPK activation. WT and AIP1-KO MLEC were treated with TLR2 ligand Pam3CSK4 (100 ng/ml, InVivoGen, San Diego, CA) for the indicated times. Phospho- and total IκBβ and p38 were determined by immunoblotting with the respective antibodies.

Fig.S2. AIP1 co-localizes with TIRAP and enhances the TIRAP-MyD88 complex. **a**. The subcellular localization of endogenous AIP1 in EC, WT or AIP1-KO MLEC were stained with anti-AIP1 antibody or a normal rabbit serum followed by Alexa Fluor 488-conjugated donkey anti-rabbit IgG. AIP1 staining was determined under fluorescence microscopy. **b-c**. AIP1 and TIRAP co-localization. BAEC and COS7 were transfected with GFP-AIP1, Flag-TIRAP (b) or together (c). TIRAP was stained with anti-Flag followed by Alexa Fluor-488 donkey anti-rabbit IgG.

Fig.S3. Mapping the lipid-binding domains on AIP1. GST-AIP1WT, AIP1 with deletion of the PH domain (AIP1ΔPH), deletion of the C2 domain (AIP1ΔC2) or deletion of both the PH and C2 domains (AIP1-C) was used for a PIP strip assay. GST was used as a control. The left panel indicates the identity of each lipid spot.

Fig.S4. AIP1 does not associate with any of the three isoforms of PIP5K. GFP-tagged PIP5Kα, β and γ) were transfected into 293T cells. The association of PIP5K with AIP1 was determined by a GST-AIP1 pulldown assay. GST was used as a control. Bound PIP5K was determined by immunoblotting with anti-GFP.

Fig.S5. a. Validation of Arf6 activity assay by GST-GGA3$_{VHS-GAT}$ pulldown. 293T cell (1X10^6) were transfected with expression plasmids for HA-tagged Arf6WT, an inactive form (Arf6T27N) or a constitutively active form (Arf6Q67L). Cell lysates were incubated with GST-GGA3$_{VHS-GAT}$ or GST beads and precipitates were analyzed by immunoblotting with an anti-Arf6 antibody. GST-GGA3$_{VHS-GAT}$ only interacts with the active Arf6-GTP form. GST fusion proteins on the membrane were visualized by staining with ponceau S. **b.** Arf1 activity is not increased in AIP1-KO cells. Arf1-GTP form from WT and AIP1-KO MLEC were determined by a GST-GGA3$_{VHS-GAT}$ pulldown assay. GST was used as a negative control. Arf6 assay was used as positive control. Input and bound Arf1 or Arf6 was determined by immunoblotting with anti-Arf1. GST and GST-GGA3$_{VHS-GAT}$ on the membrane were visualized by ponceau S staining.

Fig.S6. a. Validation of different Arf6 forms. AIP1 shows less co-localization with an inactive form of Arf6 (Arf6T27N), which is primarily in the endosomes. AIP1 and Arf6T27N expression plasmids were co-transfected into Cos7 cells. Localization of AIP1 and Arf6 was determined by indirect immunofluence microscopy with anti-Flag (AIP1) and anti-HA (Arf6) followed by Alexa Fluor-488 donkey anti-rabbit IgG and Alexa Fluor-599 donkey anti-mouse IgG. **b**. Effects of different Arf6 forms on LPS-TLR4 mediated signaling. The κB reporter gene was transfected into 293T cells with the indicated expression plasmids of Arf6 and TLR4. The TLR4 group was treated with LPS (1 ng/ml) for 8 h prior to the reporter gene assay. **b**. Alignment of AIP1 GAP domain with Arf-GAPs. Similar or identical aa were marked in black. R289 of AIP1-GAP, a residue critical for Ras-GAP activity, is absent in Arf-GAPs (marked in red).

Fig.S7. A model for the role of AIP1 in LPS-TLR4 signaling. AIP1 functions as an Arf6-GAP to negatively regulate Arf6-mediated PIP2 production, leading to normal PIP2-dependent and TIRAP-mediated formation of the TLR4-TIRAP-MyD88 complex and activation of the downstream NF-κB and MAPK signaling pathways. In AIP1-KO cells, increased active Arf6 activity leads to enhanced PIP2 production and TLR4-TIRAP-MyD88-dependent signaling.

Supplementary Figure S1

a.

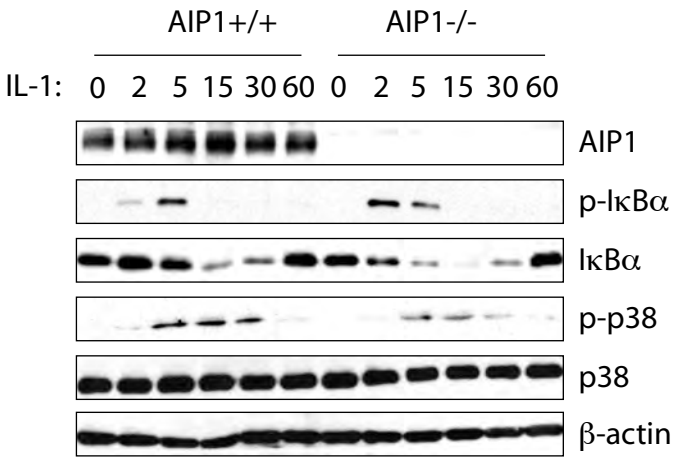

b.

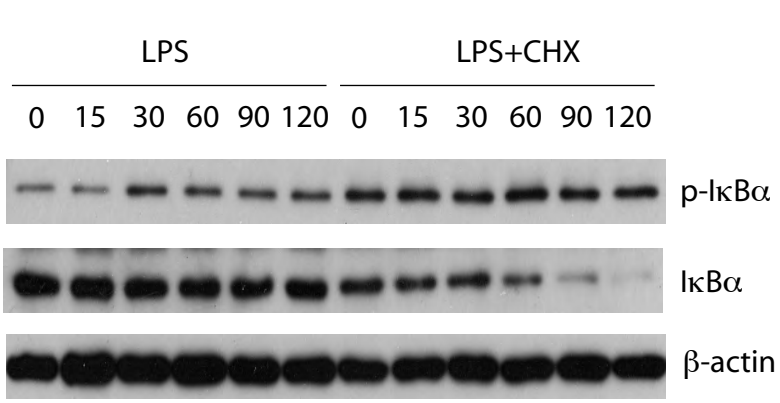

c.

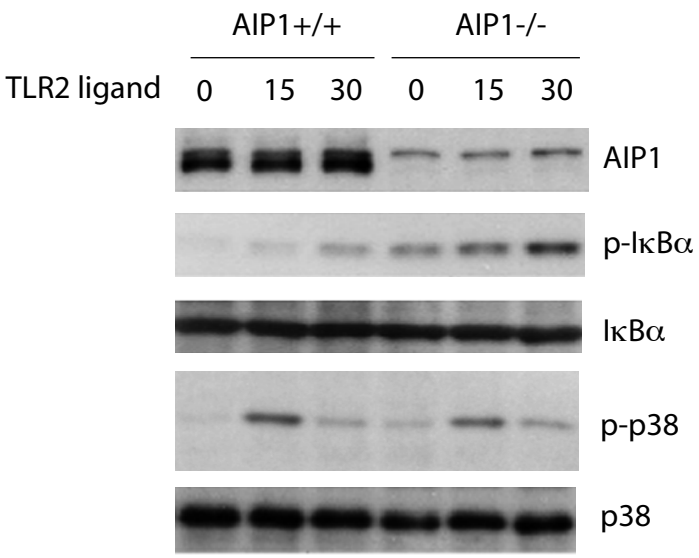

Supplementary Figure S2

a

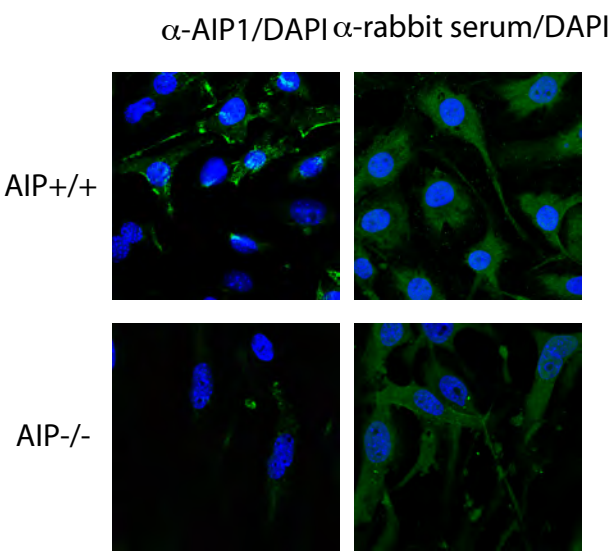

b

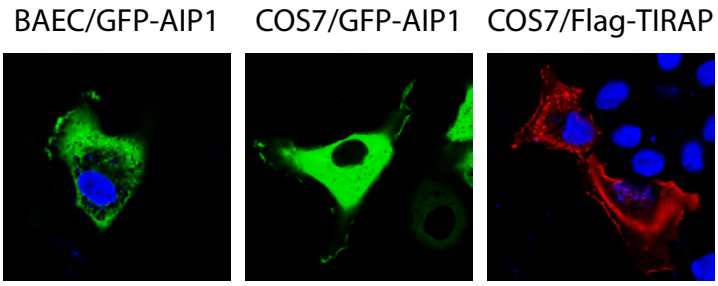

c

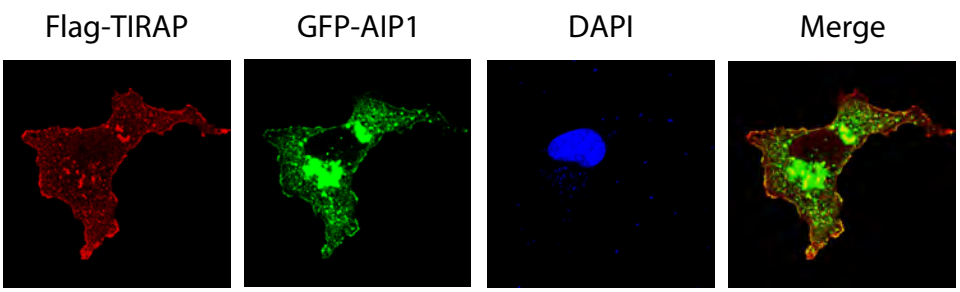

Supplementary Figure S3

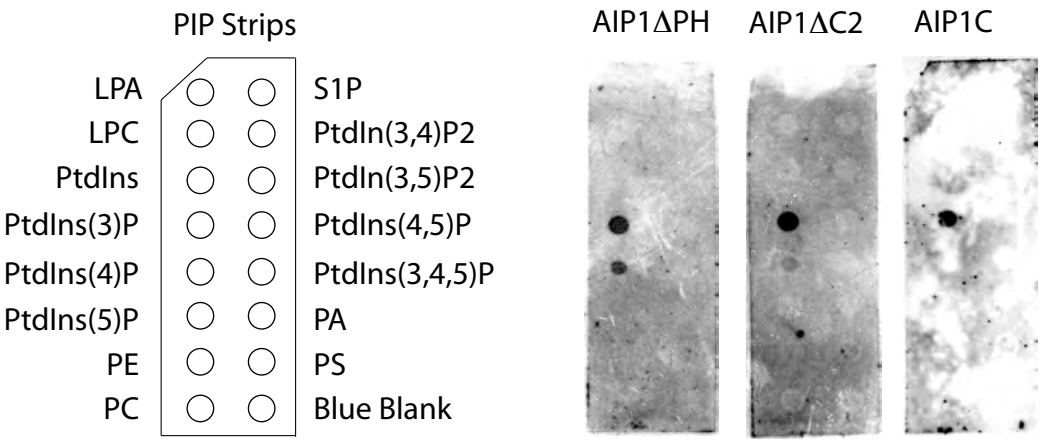

Supplementary Figure 4

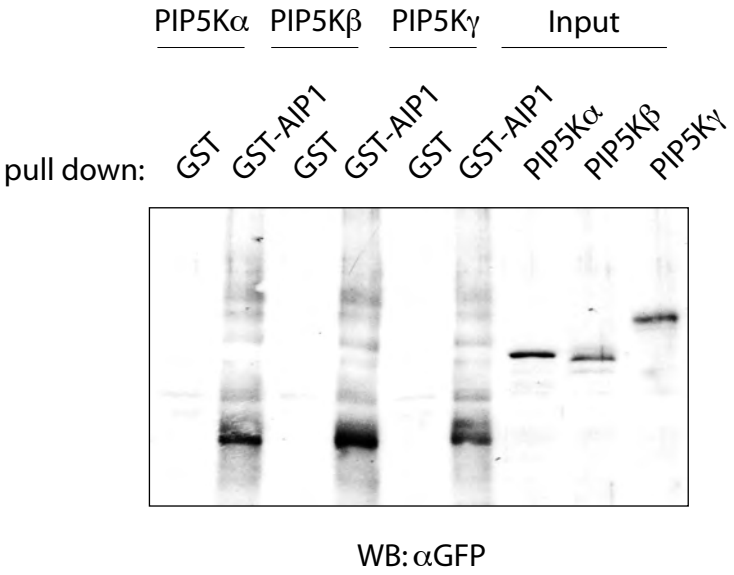

Supplementary Figure 5

a.

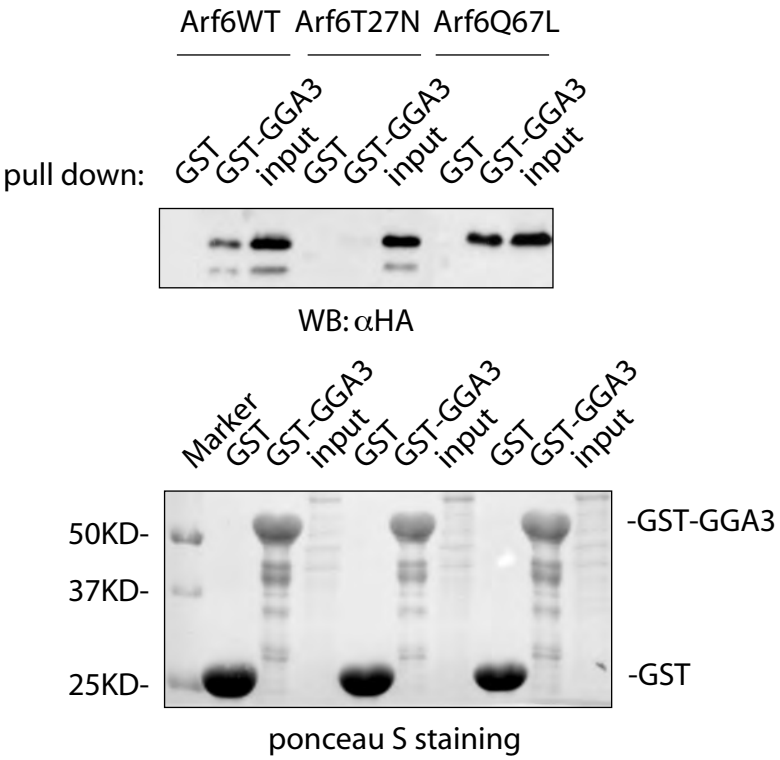

b.

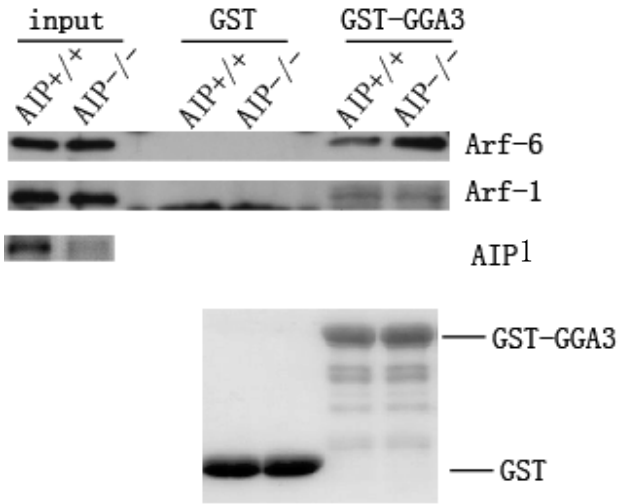

Supplementary Figure 6

a

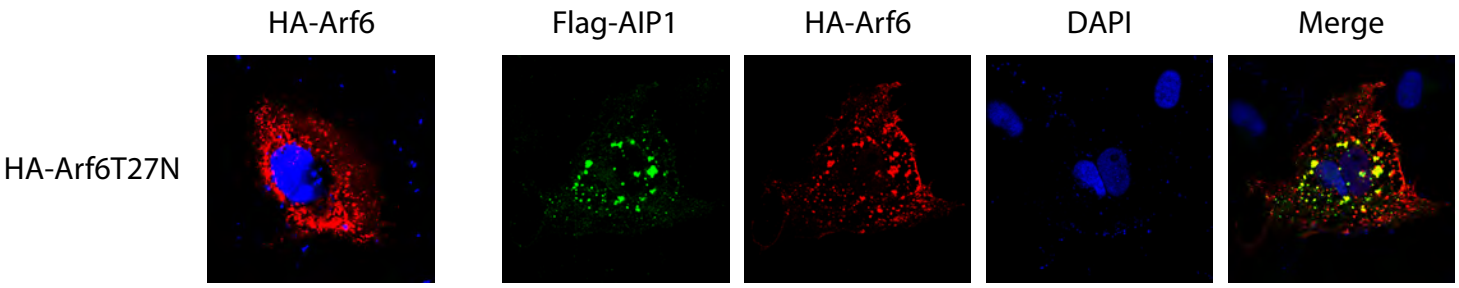

b

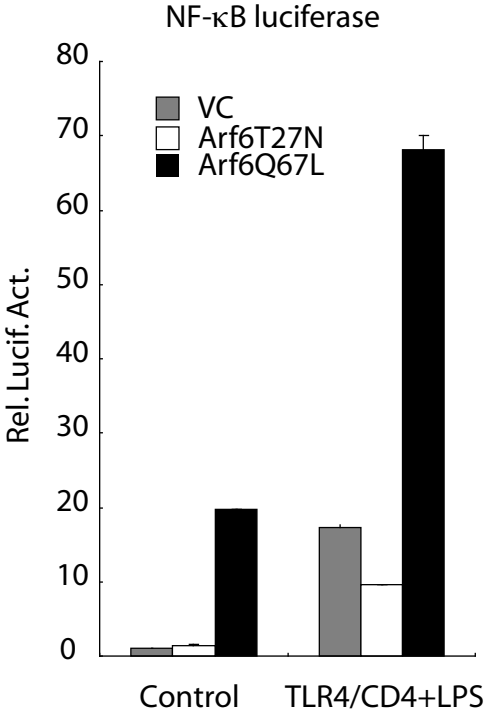

c

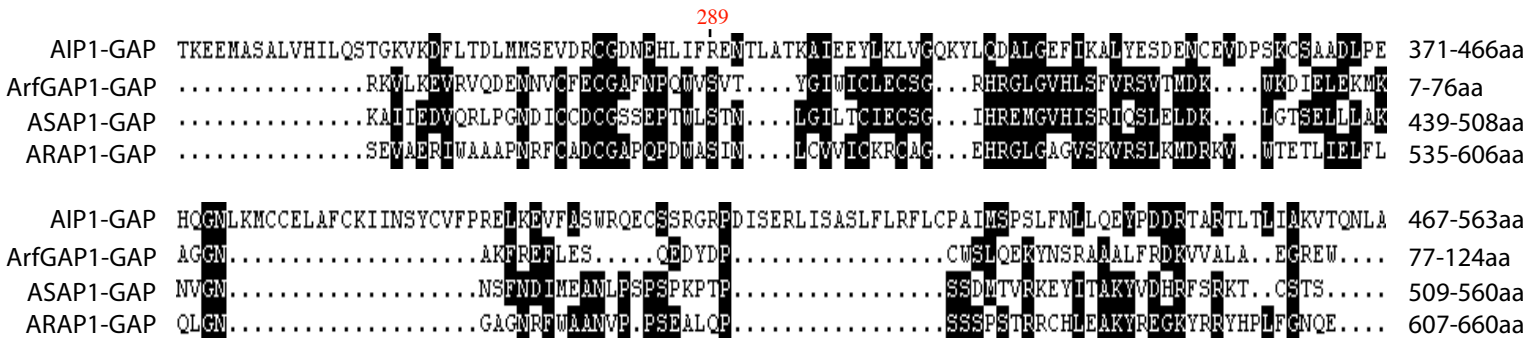

Supplementary Figure 7